



Research Paper

Autophagy inhibition attenuates hyperoxaluria-induced renal tubular oxidative injury and calcium oxalate crystal depositions in the rat kidney



Xiaolu Duan¹, Zhenzhen Kong¹, Xin Mai¹, Yu Lan, Yang Liu, Zhou Yang, Zhijian Zhao, Tuo Deng, Tao Zeng, Chao Cai, Shujue Li, Wen Zhong, Wenqi Wu*, Guohua Zeng*

Department of Urology, Minimally Invasive Surgery Center, the First Affiliated Hospital of Guangzhou Medical University, Guangdong Key Laboratory of Urology, Guangzhou Institute of Urology, China

ARTICLE INFO

Keywords:

Autophagy
Calcium oxalate stone
Oxalate
Oxidative injury
p38

ABSTRACT

Hyperoxaluria-induced oxidative injury of renal tubular epithelial cell is a casual and essential factor in kidney calcium oxalate (CaOx) stone formation. Autophagy has been shown to be critical for the regulation of oxidative stress-induced renal tubular injury; however, little is known about its role in kidney CaOx stone formation. In the present study, we found that the autophagy antagonist chloroquine could significantly attenuate oxalate-induced autophagy activation, oxidative injury and mitochondrial damage of renal tubular cells *in vitro* and *in vivo*, as well as hyperoxaluria-induced CaOx crystals depositions in rat kidney, whereas the autophagy agonist rapamycin exerted contrasting effects. In addition, oxalate-induced p38 phosphorylation was significantly attenuated by chloroquine pretreatment but was markedly enhanced by rapamycin pretreatment, whereas the protective effect of chloroquine on rat renal tubular cell oxidative injury was partly reversed by a p38 protein kinase activator anisomycin. Furthermore, the knockdown of Beclin1 represented similar effects to chloroquine on oxalate-induced cell oxidative injury and p38 phosphorylation *in vitro*. Taken together, our results revealed that autophagy inhibition could attenuate oxalate-induced oxidative injury of renal tubular cell and CaOx crystal depositions in the rat kidney *via*, at least in part, inhibiting the activation of p38 signaling pathway, thus representing a novel role of autophagy in the regulation of oxalate-induced renal oxidative injury and CaOx crystal depositions for the first time.

1. Introduction

Kidney stone is one of the most common diseases in urology and recur in up to 50% of patients within 5–10 years after the initial stone episode. Calcium-containing stones constitute approximately 80% of cases of kidney stones [1,2]. Despite the performance of an extensive number of studies, the exact mechanism responsible for kidney stone formation remains poorly understood; thus, developing effective means of preventing stone formation and recurrence remains an important challenge [3,4]. Accumulating numbers of studies have demonstrated that high oxalate- and/or CaOx-induced oxidative injury of renal tubular epithelial cell is a pivotal factor in kidney stone formation, as this type of injury not only promotes the crystallization of CaOx crystals by providing substances for their heterogeneous nucleation but also enhances the adhesion of CaOx crystals to renal epithelial cells [5–8]. Therefore, inhibiting the renal oxidative injury may have beneficial effects on renal function and decrease the rate of kidney stone

recurrence [9].

Autophagy is a cellular process that contributes to the degradation of endogenous cellular protein aggregates and damaged organelles via the lysosomal pathway and plays important roles in the pathogenesis of a variety of diseases, including kidney injury and kidney diseases [10–13]. Emerging studies recently indicated that autophagy is involved in the development of many kidney diseases, such as diabetic nephropathy, glomerular diseases, ischemia-reperfusion (I/R)-induced kidney injury, renal cancer and renal fibrosis; however, little is known about the role of autophagy in the development of kidney stones, which are a form of chronic kidney injury and disease [10,14,15]. In addition, emerging investigations have confirmed that autophagy dysfunction results in impaired mitochondrial function, reactive oxygen species (ROS) accumulation and oxidative stress [16–19].

Thus, we hypothesized that autophagy is involved in the regulation of oxalate-induced oxidative injury of renal tubular cells and investigated its role in the regulation of hyperoxaluria-induced renal

* Correspondence to: Department of Urology, Minimally Invasive Surgery Center, the First Affiliated Hospital of Guangzhou Medical University, Guangdong Key Laboratory of Urology, Kangda Road #1, Haizhu District, Guangzhou, Guangdong 510230, China.

E-mail addresses: wwqwm1@163.com (W. Wu), gzyzgh@vip.sina.com (G. Zeng).

¹ These authors contributed equally to this work.

oxidative injury and CaOx crystal depositions in the present study.

2. Materials and methods

2.1. Animal and materials

Forty male Sprague-Dawley rats (6–8 weeks old, 180–220 g) were randomly divided into the following four groups: a control group, a model group, and groups treated with rapamycin or chloroquine, respectively. The control group rats had free access to tap water. The hyperoxaluria rat model was induced by allowing the rats in the EG group free access to drinking water containing 1% EG, as described in previous studies [20–22]. The rats in the treatment groups were daily intraperitoneally injected with chloroquine (30 mg/kg/d, Sigma-Aldrich, USA) or rapamycin (0.25 mg/kg/d, Sigma-Aldrich, USA) for 4 weeks, whereas the control rats received an equal volume of normal saline. Rapamycin and chloroquine were dissolved in DMSO and PBS, respectively, as a stock solution of 10 mM, and were resuspended in saline before injection. All rats had free access to regular rat chow and were maintained at 25 °C and under a light-dark cycle during the experimental period. All procedures were performed in accordance with the Animal Management Rules of the Ministry of Health of the People's Republic of China and were approved by the Animal Care Commission of the First Affiliated Hospital of Guangzhou Medical University. Oxalate was prepared as described previously [23]. Briefly, a stock solution of 50 mM sodium oxalate was prepared in sterile PBS and was diluted to a concentration of 0.75 mM in defined medium. Anisomycin and JC-10 were purchased from Selleck and Abcam, respectively.

2.2. Cell culture and transfection

NRK-52E cells were purchased from ATCC (USA) and cultured in dulbecco's modified eagle medium (DMEM) supplemented with 10% fetal bovine serum (FBS), 1% penicillin/streptomycin and 10 mM HEPES buffer as ATCC's suggestion in a humidified incubator containing 5% CO₂ at 37 °C. The pEGFP-LC3 and ptfLC3 plasmids used in the study were gifts from Tamotsu Yoshimori (Addgene plasmid #21073 and #21074). Small interfering RNA (siRNA) was synthesized by RiBoBio Co. Ltd. (Shanghai, China). The sequences of the siRNAs used in the study were as follows: 5'-CGAUCAAUAAUUUCAGACU-3' (siRNA-Beclin-1) and 5-UUCUC CGAAGGUGUCACGU-3' (siRNA-NC). The transfections were conducted with indicated plasmids or siRNAs using Lipofectamine LTX according to the manufacturer's instructions (Invitrogen).

2.3. Cell viability assay

Cell viability was assessed using a Cell Titer 96[®] Aqueous One Solution Cell Proliferation Assay Kit (MTS, Promega). For this experiment, the cells were treated with 10 µL of MTS (5 mg/mL in PBS) and then incubated for 2 h at 37 °C in a humidified atmosphere containing 5% CO₂. Relative cell viability was assessed with an ELISA reader with a 490-nm filter.

2.4. Western blot analysis

Western blot analysis was conducted as described previously. Briefly, the cells were lysed in RIPA buffer, and equal amounts of protein were separated on an SDS polyacrylamide gel, transferred to an NC membrane (Millipore) and then immunoblotted with antibodies. Primary antibodies against the following proteins were used in this study: Beclin1 (#3495), SQSTM1/P62 (#5114), LC3A/B (#12741), phospho-p38 (T180/Y182, #4511) and p38 (#9212) were purchased from Cell Signaling Technology, 8-OHdG (ab10802) and SOD1 (ab51254) were purchased from Abcam, GAPDH (sc-365062) was purchased from Santa Cruz. The following secondary antibodies used in

the study were purchased from Santa Cruz: HRP-conjugated anti-mouse and anti-rabbit IgG (sc-2005 and sc-2004). The band intensities were quantified and normalized to the band intensities of GAPDH using ImageJ software. The data were presented as bar graphs after their statistical validity was tested.

2.5. Determination of lactate dehydrogenase (LDH) release

NRK-52E cells were seeded into 96-well plates (5 × 10³ cells/well). After the cells received the appropriate treatments, the medium from the control and experimental groups was centrifuged to remove crystals and cellular debris. LDH release was then quantified using a CytoTox 96[®] Non-Radioactive Cytotoxicity Assay Kit (Promega, USA), according to the manufacturer's instructions. The absorbance was read at 490 nm using a multimode reader (SynergyH1, BioTek), and the results were expressed as the percent LDH release. The results for the treated samples were normalized to those for the control samples.

2.6. Determination of glutathione (GSH) content

GSH content was quantified by a GloMax[®] 96 Microplate Luminometer, according to the instructions for the GSH-Glo[™] Glutathione Assay Kit (Promega, USA). The values for the treated samples were normalized to those for the control samples.

2.7. Measurement of intracellular ROS levels

Dihydroethidium (DHE) fluorescence dye was used to evaluate intracellular ROS generation. For this experiment, the cells were incubated with DHE (Sigma-Aldrich, USA) solution (5 µM) in DMEM in the dark for 30 min at 37 °C. Excess DHE was removed via two rinses with PBS solution, and the images were captured with a fluorescence microscope (IX-71, Olympus) immediately thereafter. ROS levels were semi-quantified by ImageJ software. All data pertaining to the ROS levels for the experimental group were normalized to those for the control group.

2.8. Measurement of mitochondrial membrane potential ($\Delta\psi_m$)

JC-10 dye was used to monitor mitochondrial integrity. Briefly, NRK-52E cells were seeded in black 96-well plates (1 × 10⁴ cells/well). After receiving the appropriate treatments, the cells were incubated with JC-10 (10 µg/mL) for 15 min at 37 °C and then washed twice with PBS. For signal quantification, we measured red (excitation 560 nm, emission 595 nm) and green fluorescence (excitation 485 nm, emission 535 nm) intensities using a multimode reader (Synergy H1, BioTek). Mitochondrial membrane potential ($\Delta\psi_m$) was calculated as the JC-10 red/green fluorescence intensity ratio, and this value was normalized to the corresponding value for the control group.

2.9. Transmission electron microscope (TEM) assay

Kidney tissue specimens from the rats and NRK-52E cells were fixed in 2.5% glutaraldehyde (2.5% in 0.1 M phosphate buffer, pH 7.4) and dehydrated in a graded series of ethanol. Ultrathin sections were obtained and stained as described previously [24], and then they were observed by a JEM-100CXII TEM (JEOL, Japan). The autophagosomes and autolysosomes were identified as described previously [25].

2.10. Preparation of ponceau-S-labeled COM crystals

Calcium oxalate monohydrate (COM) crystals were prepared according to protocols established previously [26]. Briefly, CaCl₂ (10 mM) and Na₂C₂O₄ (1 mM) were diluted to final concentrations of 5 mM and 0.5 mM, respectively, in Tris buffer containing 90 mM NaCl (pH 7.4) and ponceau-S (22.5 mg/mL). The mixture was incubated overnight at

room temperature, and the COM crystals were harvested by centrifugation at 2000 g for 5 min before being re-suspended in methanol and centrifuged at 2000 g for 5 min. The methanol was subsequently removed, and the COM crystals were air-dried.

2.11. Crystal-cell adhesion assay

After receiving the appropriate treatments, NRK-52E cells were cultured in a 6-well plate until they reached 100% confluence. After being washed with PBS, the cells were incubated in DMEM containing 40 $\mu\text{g}/\text{mL}$ ponceau S-labeled COM crystals for 10 min at 37 °C in a humidified atmosphere of 5% CO₂. The cells were then washed vigorously with PBS thrice to remove unbound COM crystals. Finally, pictures were captured under a Bright field inverted microscope (IX-71, Olympus), and the number of adherent (or remaining) crystals labeled by ponceau-S in at least 10 randomized high-power fields per well were counted.

2.12. Observation of renal CaOx crystal deposition

For this experiment, rat kidneys were isolated, fixed in 4% paraformaldehyde and then embedded in paraffin. Cross-sections (4 μm) of the kidneys were prepared and stained with hematoxylin-eosin, after which the sections were analyzed for COM crystal depositions via polarized light optical microphotography (CX31-P, Olympus, Japan). CaOx crystal depositions in the renal tissue sections were quantified manually by determining the sizes of the areas of crystal deposition using ImageJ software. All assessments were performed by an observer blinded to the experimental conditions.

2.13. Immunohistochemical staining

The kidney sections were processed for immunohistochemistry as described previously [27]. Antibodies against Beclin1, SQSTM1/p62,

phospho-p38, p38, 8-OHdG and SOD1 (Abcam Inc) were used for these experiments. Images were obtained with a PathScope™ 4S scanner (DigiPath, USA) and quantified using Image Pro Plus software.

2.14. Statistical analysis

The data are reported as the mean \pm SD of at least three independent experiments. The mean differences were compared using ANOVA and Student's *t*-test, and a *p* value less than 0.05 was considered statistically significant.

3. Results

3.1. Oxalate induces autophagy activation in NRK-52E cells

As high oxalate-induced oxidative stress contributes to cell injury and promotes CaOx crystal deposition renal tissues [5], we first investigated the effect of oxalate on autophagy in NRK-52E cells. As shown in Fig. 1, oxalate stimulation significantly increased Beclin1 and LC3-II expression but decreased SQSTM1/p62 expression in a time- and dose-dependent manner. TEM assay revealed that the number of autophagic vacuoles was obviously increased in the cells treated with oxalate compared with the cells in the control group (Fig. 2A). In addition, treatment with 0.75 mM oxalate clearly increased the number of LC3-II positive puncta in NRK-52E cells compared with the control group (Fig. 2B). These data indicated that oxalate stimulation could induce a significant autophagic response [28]. Furthermore, as an increase in the number of autophagic vacuoles can be caused by increased formation and/or decreased degradation of autophagic vacuoles, we investigated the effect of oxalate on autophagosome and autolysosome formation using an mRFP-GFP tandem fluorescently-tagged LC3 construct [29]. As shown in Fig. 2C, the numbers of GFP (green), mRFP (red), free mRFP (red) and yellow dots were clearly increased in the group exposed to oxalate compared with the control group, indicating an

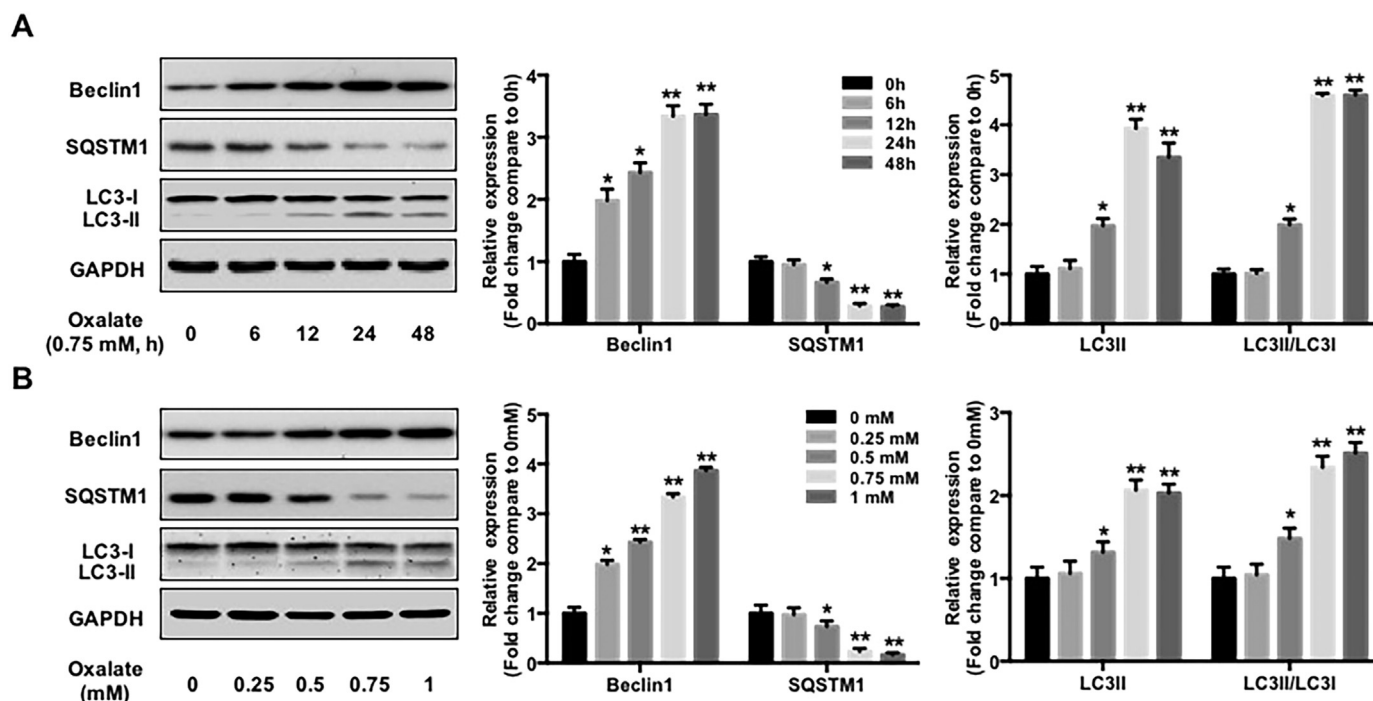


Fig. 1. Effect of oxalate stimulation on the expressions of autophagy substrates in NRK-52E cells. Twenty-four hours after seeded, NRK-52E cells were incubated in the medium supplemented with 1% FBS for 1 h, followed by the addition of oxalate (0.75 mM) for indicated hours (A) or different concentrations of oxalate for 48 h (B), then the cells were harvested and the expressions of indicated proteins were detected by western blot and quantified using ImageJ software. **P* < 0.05 and ***P* < 0.01 versus untreated group.

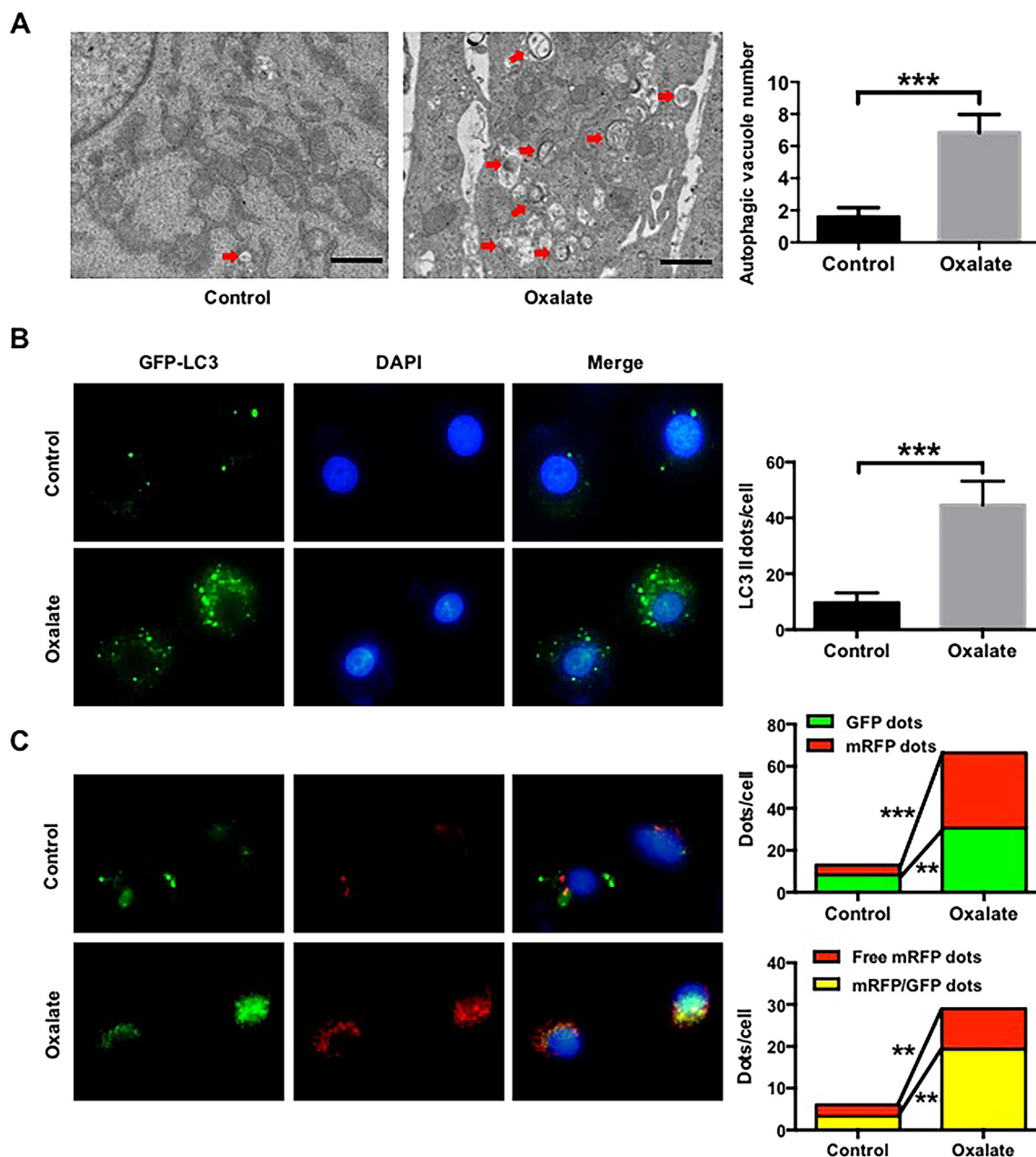


Fig. 2. Quantitative changes of autophagic vacuoles, autophagosomes and autolysosomes after exposure to urinary proteins in NRK-52E cells. (A) Quantitative changes of autophagic vacuoles under TEM in NRK-52E cells after treated with/without 0.75 mM oxalate for 48 h. The red arrows indicate autophagic vacuoles. Scale bar: 1 μ m. (B) Fluorescent microscopic and quantitative analysis of NRK-52E cells that were transfected with pEGFP-LC3 plasmids and treated with/without 0.75 mM oxalate for 48 h. (C) Fluorescent microscopic and quantitative analysis of NRK-52E cells that were transfected with pflLC3 plasmids and treated with/without 0.75 mM oxalate for 48 h. $**P < 0.01$ and $***P < 0.001$.

increase in the formation of both autophagosomes and autolysosomes after oxalate stimulation, as well as the fusion of autophagosomes and lysosomes to form autolysosomes induced by oxalate exposure.

3.2. Autophagy activation accelerates oxalate-induced oxidative injury and mitochondrial damage in NRK-52E cells

Since oxalate-induced renal cell injury is closely associated with ROS overproduction, and autophagy has been shown to regulate ROS generation and oxidative stress [7,16], we then investigated the effects of autophagy on oxalate-induced cell injury, ROS production and LDH

release in NRK-52E cells exposed to oxalate in the presence of rapamycin (an autophagy agonist) or chloroquine (an autophagy antagonist). As shown in Fig. 3A, oxalate-induced inhibition of cell viability was significantly attenuated in the presence of chloroquine, whereas cell viability decreased further in the presence of rapamycin. In addition, chloroquine pretreatment clearly attenuated oxalate-induced ROS generation, LDH release and GSH decrease, whereas rapamycin represented contrasting effects (Figs. 3B–3D). Since the mitochondrial respiratory chain is the major source of ROS in the kidney [30,31], we then detected the effect of autophagy on oxalate-induced mitochondrial damage. As shown in Fig. 3E, chloroquine pretreatment obviously

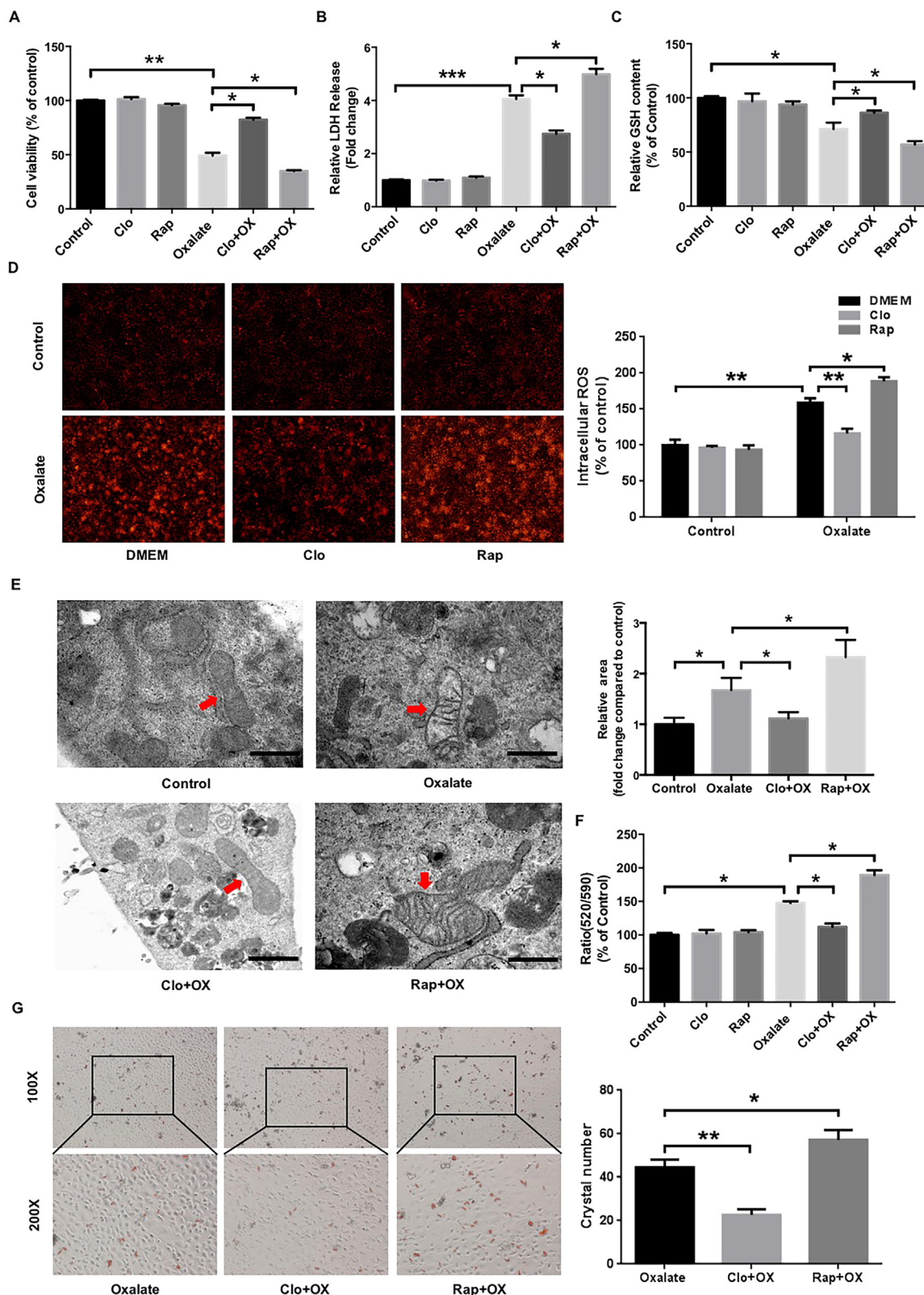


Fig. 3. Effects of rapamycin and chloroquine on oxalate-induced oxidative injury of NRK-52E cells. (A-C) Twenty-four hours after being seeded in a 96-well plate, NRK-52E cells were incubated with or without rapamycin (RAP, 5 μ M) or chloroquine (Clo, 5 μ M) for 2 h, after which they were stimulated with oxalate (0.75 mM) for 48 h. Cell viability, LDH release and GSH release were subsequently assessed as described in the “Materials and Methods”. (D) DHE staining results and quantitative data for cells treated as described in (A-C). (E) Ultrastructural images of the mitochondria in NRK-52E cells treated as described above. Scale bar: 500 nm. The surface areas of indicated mitochondria were quantified using ImageJ software. (F) Mitochondrial membrane potential ($\Delta\psi_m$) of the cells treated as described above was determined by JC-10 assay. (G) Crystal-cell adhesion assay results and quantitative data for ponceau-S-labeled COM crystals (red) adhering to cells treated as described above. Original magnification 200 \times . * P < 0.05, ** P < 0.01 and *** P < 0.001.

attenuated oxalate-induced mitochondria edema and damage, whereas rapamycin significantly enhanced the injury. In addition, chloroquine significantly attenuated the mitochondrial membrane potential ($\Delta\psi_m$) losses induced by oxalate, whereas rapamycin represented a contrasting effect (Fig. 3F). Furthermore, the adhesion of CaOx crystals to injured renal tubular epithelial cells is a key step in the development of kidney stones [5,32,33]; thus, we investigated the effect of autophagy on crystal adhesion and found that chloroquine significantly decreased the adhesion of CaOx crystals to NRK-52E cells, whereas rapamycin clearly enhanced the adhesion (Fig. 3G). Together, these results suggested that autophagy activation accelerates oxalate-induced oxidative injury and mitochondrial damage in NRK-52E cells and promotes the adhesion of CaOx crystals to injured cells.

3.3. p38 signaling is involved in autophagy-mediated oxidative injury induced by oxalate in NRK-52E cells

Since p38 protein kinase is a pivotal signal protein that promotes ROS generation and oxidative injury after being activated in response to oxidative stress, we then investigated the effect of autophagy on p38 activation. The results revealed that chloroquine clearly attenuated oxalate-induced p38 phosphorylation, whereas rapamycin significantly enhanced oxalate-induced p38 phosphorylation (Figs. 4A and 4B). In addition, anisomycin, a chemical activator of p38 [34], partially reversed the effects of chloroquine on oxalate-induced p38 phosphorylation, cell viability inhibition, LDH release, ROS generation and membrane potential losses, whereas had no significant effect on chloroquine-mediated ratio of LC3 II/LC3 I (Figs. 4C–4G). Taken together, these results indicated that chloroquine-mediated protective effect on oxalate-induced oxidative injury and mitochondrial damage is, at least in part, mediated by p38 signaling.

3.4. Beclin1 siRNA-mediated autophagy inhibition protects NRK-52E cells from oxalate-induced oxidative injury

Furthermore, the role of autophagy in the regulation of oxalate-induced oxidative injury was confirmed by knocking down Beclin1 expression in NRK-52E cells (Fig. 5A). Similar to chloroquine pretreatment, Beclin1 siRNA also attenuated the effects of oxalate on p38 phosphorylation, cell viability, ROS generation and LDH release in NRK-52E cells (Figs. 5A–5D), suggesting that autophagy inhibition has protective effects on oxalate-induced oxidative injury in renal tubular epithelial cells.

3.5. Autophagy inhibition attenuates ethylene glycol (EG)-induced oxidative stress-mediated injury and CaOx crystal deposition in the rat kidney

Finally, a hyperoxaluria rat model induced by EG was used to assess the effects of oxalate on renal tubular epithelial cell injury and CaOx crystal depositions in vivo [27]. TEM assay showed that the number of autophagic vacuoles, including autophagosome and autolysosome, is significantly increased in model rats compared with control rats (Fig. 6A). Immunohistochemistry assay showed that Beclin1 protein expression levels were significantly increased, and SQSTM1 expression levels were decreased in the kidneys of EG-treated rats compared with the kidneys of control rats (Fig. 6B). Administration of chloroquine or rapamycin induced changes in SQSTM1 and Beclin1 expression similar to those seen in the cell-based experiments, indicating that hyperoxaluria-induced autophagy is modulated by rapamycin and chloroquine in EG-treated rats. Meanwhile, EG-induced CaOx crystal depositions in the rat kidney were almost completely disappeared in the rats treated with chloroquine, whereas rapamycin treatment markedly increased

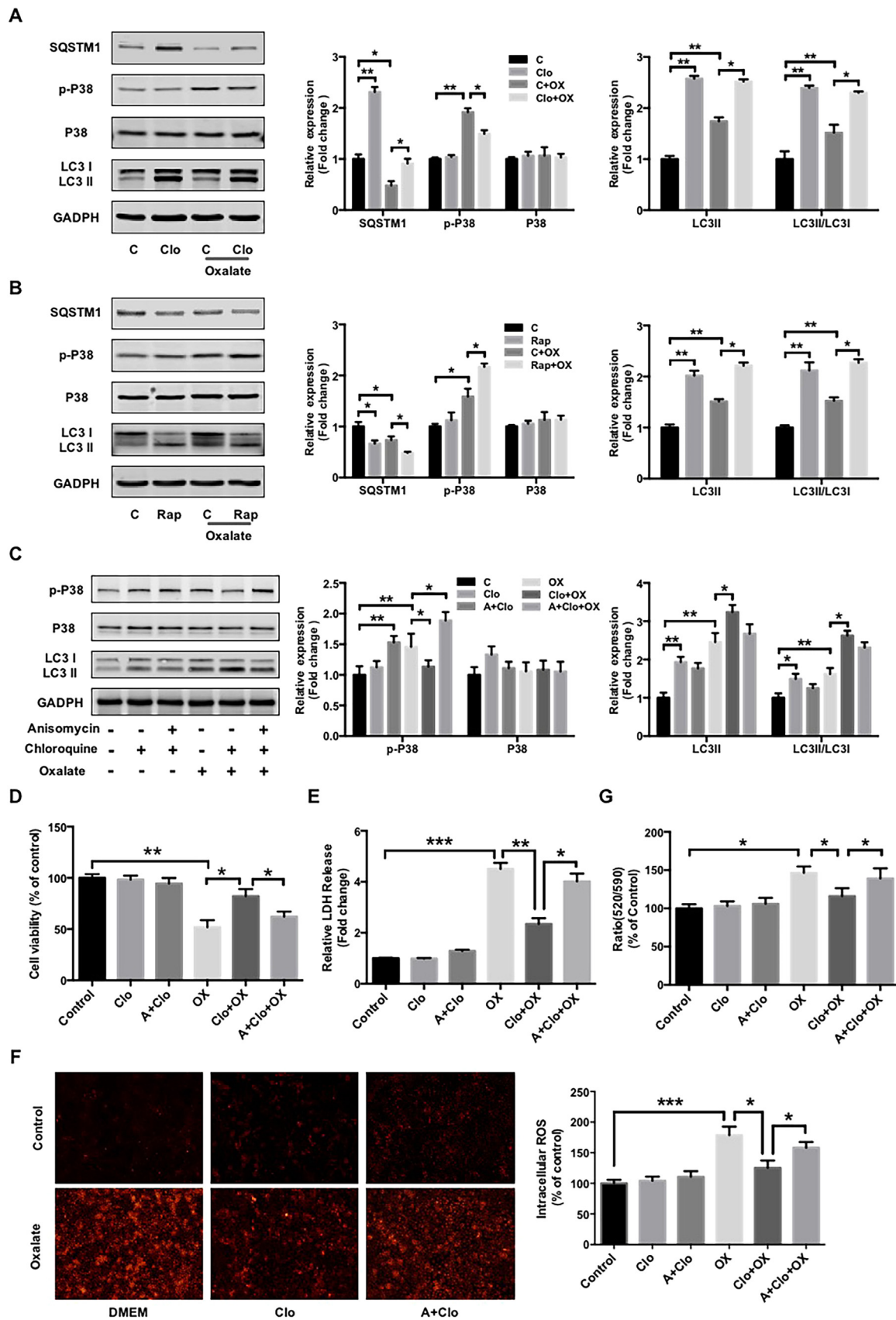
the crystal depositions (Fig. 6C). In addition, chloroquine treatment significantly attenuated renal tubular injury, as determined by assessments of the release of renal tubular injury markers, such as SOD1 and 8-OHdG, and mitochondrial damage. In contrast, rapamycin treatment increased the 8-OHdG expression and mitochondrial damage (Figs. 7A and 7B). Furthermore, similar to the results of cell-based experiments, the phosphorylation and expression of p38 in EG-treated rat kidneys were clearly increased compared with that in control rat kidneys, and these increases were significantly attenuated by chloroquine treatment but was markedly enhanced by rapamycin treatment (Fig. 7A), demonstrating that chloroquine-mediated autophagy inhibition plays a protective role in hyperoxaluria-induced renal tubular epithelial cell injury and CaOx crystals depositions.

4. Discussion

In the present study, we found that oxalate stimulation activated autophagy in renal tubular epithelial cells and chloroquine pretreatment significantly attenuated oxalate-induced mitochondrial damage and oxidative injury, as well as EG-induced CaOx crystals depositions in the rat kidney, via, at least in part, inhibiting p38 signaling activation in vitro and in vivo, whereas rapamycin had contrasting effects, revealing a novel role of autophagy in the regulation of oxalate-induced oxidative injury of renal tubular cell and EG-induced CaOx crystals depositions in the rat kidney.

Kidney stone is a type of chronic kidney injury, and emerging investigations have indicated that autophagy plays important roles in the regulation of both acute kidney injury (AKI) and chronic kidney diseases (CKDs), such as I/R-induced kidney injury, sepsis, nephrotoxin-induced AKI, glomerular disease, diabetic nephropathy and renal fibrosis; however, little is known about the role of autophagy in the regulation of kidney stone formation [10,11]. To investigate the role of autophagy in the regulation of oxalate-induced renal tubular cell injury and renal stone formation, we first examined the effect of oxalate exposure on autophagy activation in renal tubular epithelial cells and found that oxalate stimulation could regulate the molecular markers' expressions of autophagy activation in a time- and dose-dependent manner, such as Beclin1, LC3 II/LC3 I and SQSTM1. TEM assay and LC3-II positive puncta detection also confirmed that autophagy is activated in response to oxalate stimulation. In addition, both the numbers of autophagosomes and autolysosomes were dramatically increased in the oxalate-treated cell compared with the untreated cells. Taken together, these data strongly indicated that autophagy was activated in response to oxalate stimulation in renal tubular epithelial cells, which is similar to the effect of urinary proteins exposure [25,28].

Since the oxidative injury of renal tubular cells induced by high oxalate and/or CaOx crystals is a key factor in stone formation [5], we then detected the effects of autophagy activation and inhibition, which were induced by rapamycin and chloroquine, respectively, on oxalate-induced cell oxidative injury in NRK-52E cells. Interestingly, the results showed that chloroquine pretreatment significantly attenuated oxalate-induced cell viability inhibition and oxidative injury, whereas rapamycin exerted contrasting effects, indicating that autophagy activation has detrimental effects on cells exposed to oxalate, these results are opposite to the results of urinary proteins, cisplatin and cyclosporine A exposure. In one hand, autophagy was found to proceed cell apoptosis and injury under a low level of injury via clearing the degradation of damaged subcellular organelles, whereas severe injury-induced excessive autophagy activation may be detrimental [35–37]. In another hand, the effect of autophagy activation on cell death and injury is related to its duration. For example, unilateral ureteral obstruction (UUO)-induced autophagy has a protective role at an early stage but persistent UUO stimulation induces proximal tubular epithelial cell



(caption on next page)

Fig. 4. Involvement of p38 signaling in the regulation of autophagy-mediated oxidative injury induced by oxalate. (A and B) The expression levels of indicated proteins in NRK-52E cells treated as described in Fig. 3A were detected by western blot and quantified using ImageJ software. (C) Twenty-four hours after being seeded in 60-mm dishes, the cells were incubated with or without anisomycin (A, 1 μ M) for 2 h, after which they were treated with or without chloroquine (Clo, 5 μ M) for 2 h and stimulated with oxalate (0.75 mM) for 48 h. The expression levels of the indicated proteins were detected by western blot and quantified using ImageJ software. (D, E and G) NRK-52E cells were seeded in a 96-well plate and treated as described in (B), then the cell viability, LDH release and mitochondrial membrane potential were assessed as described in Fig. 3. (F) DHE staining results and quantitative data for cells treated as described in (C). Original magnification 200 \times . * P < 0.05, ** P < 0.01 and *** P < 0.001.

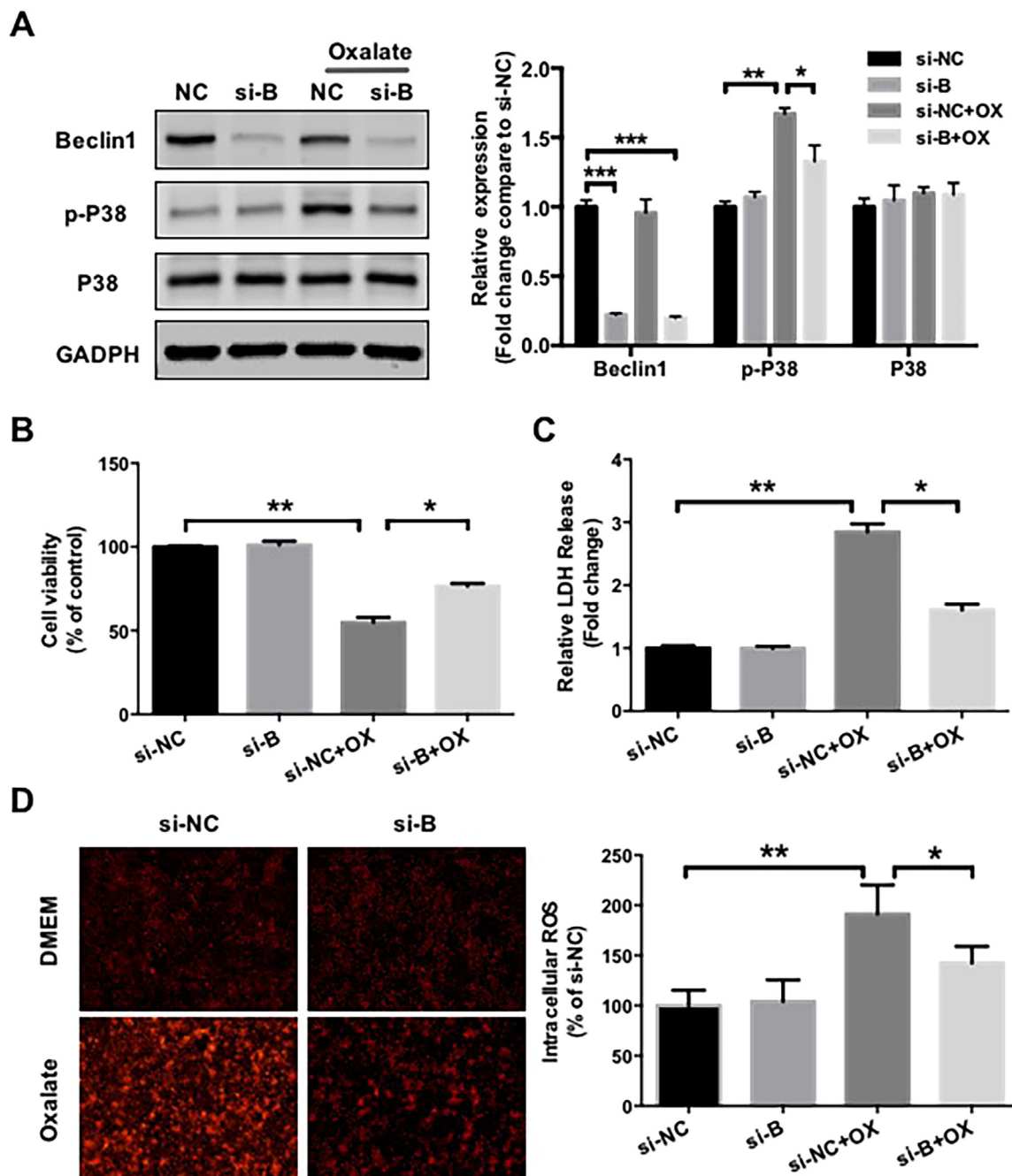


Fig. 5. Effects of siRNA-mediated Beclin1 knockdown on oxalate-induced oxidative injury in NRK-52E cells. (A) Forty-eight hours after transfection, NRK-52E cells were cultured in medium supplemented with or without 0.75 mM oxalate for 48 h, then the expressions of indicated proteins were detected by western blot and quantified using ImageJ software. (B and C) Forty-eight hours after transfection, equal amounts of cells were seeded in 96-well plate and cultured in medium supplemented with or without 0.75 mM oxalate for 48 h. Cell viability and LDH release were subsequently assessed. (D) DHE staining results and quantitative data for cells treated as described in (A). Original magnification 200 \times . * P < 0.05 and ** P < 0.01.

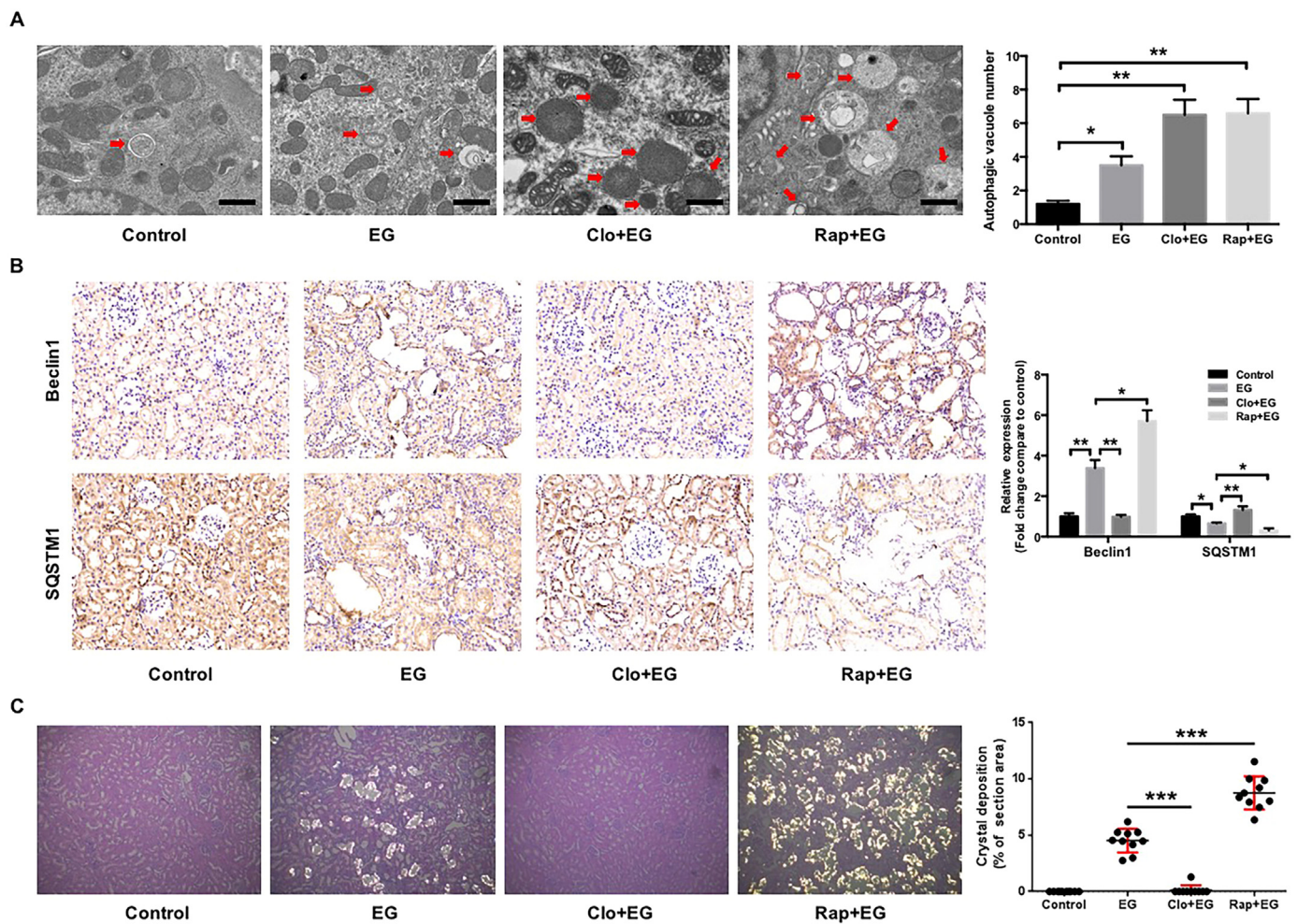


Fig. 6. Effects of rapamycin or chloroquine on autophagic activity and EG-induced CaOx crystals depositions in rat kidneys. (A) Quantitative changes in autophagic vacuoles under TEM in kidney sections from indicated rats. The red arrows indicate autophagic vacuoles. Scale bar: 1 μ m. (B) The expressions of Beclin1 and SQSTM1 in kidney sections from indicated rats were detected by immunohistochemical staining and quantified using Image Pro Plus software. (magnification 200 \times) (C) Photomicrographs of kidney sections from indicated rats were obtained under dark field illumination with polarized light. Retained crystals exhibit strong birefringence (magnification 200 \times). The sizes of the areas of crystal deposition per field were estimated and quantified using ImageJ software. * P < 0.05, ** p < 0.01 and *** p < 0.001.

death by excessive autophagy activation and oxidative stress in the obstructed kidney [38]. So, we supposed that the different effects of autophagy on renal tubular epithelial cell injury, which were induced by oxalate, urinary proteins, cisplatin or cyclosporine A, may be caused by the different levels of injury and duration of autophagy activation. In addition, though autophagy has been shown to be involved in AKI and CKD development, its role in the regulation of renal cell injury remains a controversial subject [10]. Some studies reported that autophagy activation protects renal tubular epithelial cells from injury induced by cisplatin, cyclosporine A or urinary proteins [25]. In contrast, some other studies indicated that increased autophagic activity contributes to renal tubular epithelial cell death in I/R- or tunicamycin-induced renal injury [39]. Therefore, whether autophagy activation has protective or detrimental effects on renal tubular epithelial cells maybe stress factor or autophagy duration dependent. However, the mechanism driving the transition of the effects of autophagy from protective to detrimental needs further investigation. Furthermore, the adhesion of crystals to renal epithelial cells, which is a key step in renal stone formation [1–3], was markedly attenuated by chloroquine but was enhanced by rapamycin, suggesting that persistent autophagy activation may have a

detrimental role during renal CaOx stone formation.

The mitochondrial respiratory chain is the principal source of ROS in the kidney, and mitochondrial function, integrity and membrane potential drive the generation of ROS, which are the key cause of oxalate- and/or CaOx-induced oxidative stress-mediated renal tubular cell injury. Previous studies have shown that autophagy plays an important role in the regulation of mitochondrial turnover, function, integrity and intracellular protein clearance, and disruption of the early steps of the autophagy pathway usually results in ubiquitinated protein accumulation, increased ROS generation and mitochondrial dysfunction [16,40]. In contrast, in the present study our results indicated that oxalate-induced mitochondrial edema and depolarization, as well as the oxidative injury of renal tubular cells, were markedly attenuated by chloroquine pretreatment but accelerated by rapamycin pretreatment, suggesting that autophagy activation has detrimental effects on oxalate-induced mitochondrial damage and oxidative injury in renal tubular epithelial cells. In general, autophagy activation reduces ROS formation and oxidative injury via promoting mitophagy, but we noticed that the injury usually is light or acute, such as urinary proteins or I/R-induced injury, which is different from the injury induced by oxalate in the

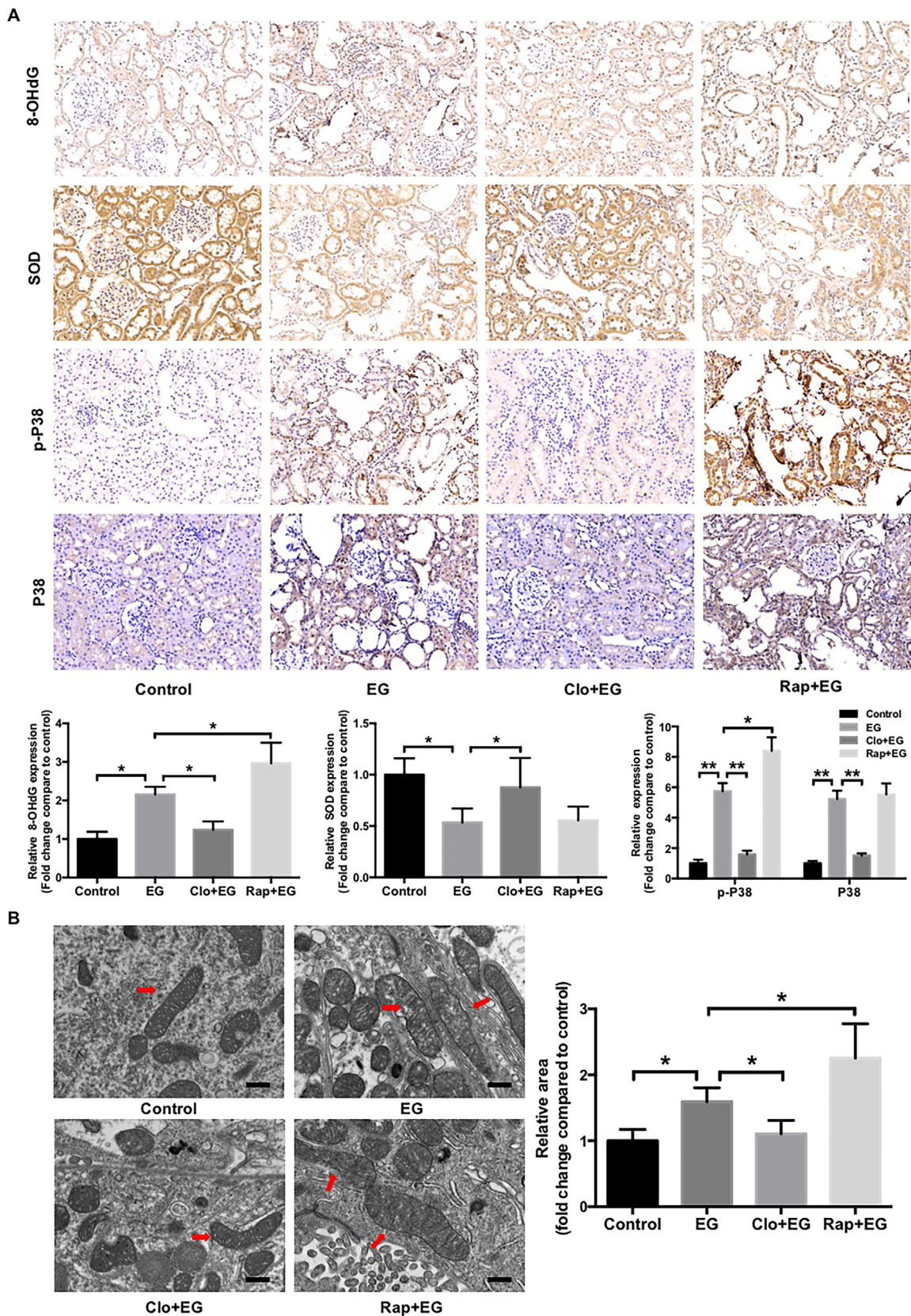


Fig. 7. Effects of rapamycin or chloroquine on EG-induced renal oxidative injury in rat kidneys. (A) Immunohistochemical staining and quantification for oxidative injury-related markers and p38 in kidney sections from indicated rats. Original magnification 200 ×. (B) Ultrastructural images of mitochondria in kidney sections from indicated rats. The red arrows indicate mitochondria. Scale bar: 500 nm. The surface areas of indicated mitochondria were quantified using ImageJ software. **P* < 0.05, ***P* < 0.01 versus Control group, # *P* < 0.05, ##*P* < 0.01 versus EG group.

present study, thus, we supposed that the effects of autophagy on mitochondrial damage and oxidative injury may be depended on the injury type and autophagy duration.

Then we investigated the mechanism responsible for autophagy-related cell injury induced by oxalate and found that chloroquine significantly attenuated oxalate-induced phosphorylation of p38, a key protein kinase that promotes oxidative stress-induced ROS generation and tissue injury after its phosphorylation, whereas rapamycin clearly enhanced the phosphorylation of p38. In addition, the effects of chloroquine on oxalate-induced mitochondrial depolarization and oxidative injury were partly reversed by pretreatment with anisomycin, an agonist of the p38 signaling. Though chloroquine had been demonstrated to activate tyrosine kinase and/or PKC to induce p38 MAPK activation, which in turn induces iNOS expression and NO production, but the concentration of chloroquine used in the study is much higher than that used in the present study (100 μ M vs 5 μ M) [41]. Similar to our results, a recent research revealed that chloroquine suppresses Kaposi's sarcoma-associated herpesvirus-induced p38 activation [42]. Since the side-effects of chloroquine in clinical use is related to its dose, we supposed that the distinct effects of chloroquine on p38 signaling activation is caused by the different concentration. Furthermore, Beclin1 siRNA-mediated autophagy inhibition represented similar effects to chloroquine on oxalate-induced oxidative injury and p38 signaling activation in NRK-52E cells, suggesting that the protective effect of autophagy inhibition, which was induced by chloroquine or Beclin1 siRNA, on oxalate-induced oxidative injury of renal tubular epithelial cells is mediated, at least in part, by p38 MAPK signaling.

Finally, we confirmed the role of autophagy in the regulation of oxalate-induced renal injury and CaOx stone formation in vivo using an EG-treated rat model, a classic model that is widely used in studies about hyperoxaluria-induced renal injury and renal stone formation. Our data revealed that hyperoxaluria-induced oxidative injury of renal tubular cells and mitochondria, as well as CaOx crystals depositions, were significantly alleviated by chloroquine but were enhanced by rapamycin. These results were consistent with the data from the cell experiments and confirmed that autophagy activation promotes renal stone formation. Furthermore, chloroquine has been used to treat malaria and autoimmune diseases for several decades and, more recently, has been used to potentiate cancer chemotherapies and is very safe but has a plethora of dose-dependent effects. Since the human dose (4.76 mg/kg/day) equivalent to the rat dose used in the present study is much lower than the maximum dose (less than 10 mg/kg/day) that is safe for human, as determined by previous research [43], we anticipate that appropriate use of chloroquine may greatly and safely decrease the rate of CaOx nephrolithiasis recurrence; however, further studies about the exact role and underlying mechanism of chloroquine in the regulation of renal CaOx stone formation are still needed.

In conclusion, our results demonstrated for the first time that oxalate-induced persistent autophagy activation is a detrimental response that accelerates renal tubular epithelial cell oxidative injury in vitro and in vivo, thus revealing a novel role of autophagy in the regulation of renal oxidative injury and CaOx crystals depositions induced by oxalate stimulation, and suggesting that chloroquine may be indicated as a treatment for CaOx nephrolithiasis and inhibiting autophagy activation in renal tubular epithelial cells may be beneficial in the clinical management of CaOx nephrolithiasis.

Acknowledgements

This work was financed by grants from the Guangzhou Science Technology and Innovation Commission (No. 201607010162, No. 201604020001 and No. 201704020193), the National Natural Science Foundation of China (No. 81670643 No. 81600542 and No. 81570633) and the Collaborative Innovation Project of Guangzhou Education Bureau (No. 1201620011).

Declarations of interest

There are no interests to declare.

References

- [1] S. Kusmartsev, P.R. Dominguez-Gutierrez, B.K. Canales, V.G. Bird, J. Vieweg, S.R. Khan, Calcium oxalate stone fragment and crystal phagocytosis by human macrophages, *J. Urol.* 195 (2016) 1143–1151, <http://dx.doi.org/10.1016/j.juro.2015.11.048>.
- [2] G. Zeng, Z. Mai, S. Xia, Z. Wang, K. Zhang, L. Wang, Y. Long, J. Ma, Y. Li, S.P. Wan, W. Wu, Y. Liu, Z. Cui, Z. Zhao, J. Qin, T. Zeng, Y. Liu, X. Duan, X. Mai, Z. Yang, Z. Kong, T. Zhang, C. Cai, Y. Shao, Z. Yue, S. Li, J. Ding, S. Tang, Z. Ye, Prevalence of kidney stones in China: an ultrasonography based cross-sectional study, *BJU Int.* 120 (2017) 109–116, <http://dx.doi.org/10.1111/bju.13828>.
- [3] A.P. Evan, E.M. Worcester, F.L. Coe, J. Williams, J.E. Lingeman, Mechanisms of human kidney stone formation, *Urolithiasis* 43 (Suppl. 1) (2015) 19–32, <http://dx.doi.org/10.1007/s00240-014-0701-0>.
- [4] E.M. Worcester, F.L. Coe, Clinical practice. Calcium kidney stones, *N. Engl. J. Med.* 363 (2010) 954–963, <http://dx.doi.org/10.1056/NEJMcp1001011>.
- [5] K.P. Aggarwal, S. Narula, M. Kakkur, C. Tandon, Nephrolithiasis: molecular mechanism of renal stone formation and the critical role played by modulators, *BioMed. Res. Int.* 2013 (2013) 292953, <http://dx.doi.org/10.1155/2013/292953>.
- [6] S.R. Khan, Is oxidative stress, a link between nephrolithiasis and obesity, hypertension, diabetes, chronic kidney disease, metabolic syndrome? *Urol. Res.* 40 (2012) 95–112, <http://dx.doi.org/10.1007/s00240-011-0448-9>.
- [7] S.R. Khan, Reactive oxygen species as the molecular modulators of calcium oxalate kidney stone formation: evidence from clinical and experimental investigations, *J. Urol.* 189 (2013) 803–811, <http://dx.doi.org/10.1016/j.juro.2012.05.078>.
- [8] B. Hoppe, An update on primary hyperoxaluria, *Nat. Rev. Nephrol.* 8 (2012) 467–475, <http://dx.doi.org/10.1038/nrneph.2012.113>.
- [9] M. Davalos, S. Konno, M. Eshghi, M. Choudhury, Oxidative renal cell injury induced by calcium oxalate crystal and renoprotection with antioxidants: a possible role of oxidative stress in nephrolithiasis, *J. Endourol.* 24 (2010) 339–345, <http://dx.doi.org/10.1089/end.2009.0205>.
- [10] Z. Wang, M.E. Choi, Autophagy in kidney health and disease, *Antioxid. Redox Signal.* 20 (2014) 519–537, <http://dx.doi.org/10.1089/ars.2013.5363>.
- [11] Y. Takabatake, T. Kimura, A. Takahashi, Y. Isaka, Autophagy and the kidney: health and disease, *Nephrol. Dial. Transplant. Off. Publ. Eur. Dial. Transpl. Assoc. - Eur. Ren. Assoc.* 29 (2014) 1639–1647, <http://dx.doi.org/10.1093/ndt/gft535>.
- [12] S. Sridhar, Y. Botbol, F. Macian, A.M. Cuervo, Autophagy and disease: always two sides to a problem, *J. Pathol.* 226 (2012) 255–273, <http://dx.doi.org/10.1002/path.3025>.
- [13] B. Levine, G. Kroemer, Autophagy in the pathogenesis of disease, *Cell* 132 (2008) 27–42, <http://dx.doi.org/10.1016/j.cell.2007.12.018>.
- [14] T.B. Huber, C.L. Edelstein, B. Hartleben, K. Inoki, M. Jiang, D. Koya, S. Kume, W. Lieberthal, N. Pallet, A. Quiroga, K. Ravichandran, K. Susztak, S. Yoshida, Z. Dong, Emerging role of autophagy in kidney function, diseases and aging, *Autophagy* 8 (2012) 1009–1031, <http://dx.doi.org/10.4161/auto.19821>.
- [15] S.R. Mulay, J.N. Eberhard, J. Desai, J.A. Marschner, S.V.R. Kumar, M. Weidenbusch, M. Grigorescu, M. Lech, N. Eltrich, L. Müller, W. Hans, M. Hrabě de Angelis, V. Vielhauer, B. Hoppe, J. Asplin, N. Burzlauff, M. Herrmann, A. Evan, H.-J. Anders, Hyperoxaluria requires TNF receptors to initiate crystal adhesion and kidney stone disease, *J. Am. Soc. Nephrol. JASN* 28 (2017) 761–768, <http://dx.doi.org/10.1681/ASN.2016040486>.
- [16] J. Lee, S. Giordano, J. Zhang, Autophagy, mitochondria and oxidative stress: cross-talk and redox signalling, *Biochem. J.* 441 (2012) 523–540, <http://dx.doi.org/10.1042/BJ20111451>.
- [17] T. Kimura, A. Takahashi, Y. Takabatake, T. Namba, T. Yamamoto, J.-Y. Kaimori, I. Matsui, H. Kitamura, F. Niimura, T. Matsusaka, T. Soga, H. Rakugi, Y. Isaka, Autophagy protects kidney proximal tubule epithelial cells from mitochondrial metabolic stress, *Autophagy* 9 (2013) 1876–1886, <http://dx.doi.org/10.4161/auto.25418>.
- [18] T. Kawakami, I.G. Gomez, S. Ren, K. Hudkins, A. Roach, C.E. Alpers, S.J. Shankland, V.D. D'Agati, J.S. Duffield, Deficient autophagy results in mitochondrial dysfunction and FSGS, *J. Am. Soc. Nephrol. JASN* 26 (2015) 1040–1052, <http://dx.doi.org/10.1681/ASN.2013111202>.
- [19] R. Scherz-Shouval, Z. Elazar, ROS, mitochondria and the regulation of autophagy, *Trends Cell Biol.* 17 (2007) 422–427, <http://dx.doi.org/10.1016/j.tcb.2007.07.009>.
- [20] K. Taguchi, A. Okada, T. Yasui, T. Kobayashi, R. Ando, K. Tozawa, K. Kohri, Pioglitazone, a peroxisome proliferator activated receptor γ agonist, decreases renal crystal deposition, oxidative stress and inflammation in hyperoxaluric rats, *J. Urol.* 188 (2012) 1002–1011, <http://dx.doi.org/10.1016/j.juro.2012.04.103>.
- [21] E. Letavernier, C. Verrier, F. Goussard, J. Perez, L. Huguet, J.-P. Haymann, L. Baud, D. Bazin, M. Daudon, Calcium and vitamin D have a synergistic role in a rat model of kidney stone disease, *Kidney Int.* 90 (2016) 809–817, <http://dx.doi.org/10.1016/j.kint.2016.05.027>.
- [22] R.R. Hoopes, R. Reid, S. Sen, C. Szpirer, P. Dixon, A.A.J. Pannett, R.V. Thakker, D.A. Bushinsky, S.J. Scheinman, Quantitative trait loci for hypercalcaemia in a rat model of kidney stone disease, *J. Am. Soc. Nephrol. JASN* 14 (2003) 1844–1850.
- [23] V. Thamilselvan, M. Menon, S. Thamilselvan, Oxalate-induced activation of PKC- α and δ regulates NADPH oxidase-mediated oxidative injury in renal tubular epithelial cells, *Am. J. Physiol. Ren. Physiol.* 297 (2009) F1399–F1410, <http://dx.doi.org/10.1152/ajprenal.00051.2009>.

- [24] W.J. Liu, S.H. Xie, Y.N. Liu, W. Kim, H.Y. Jin, S.K. Park, Y.M. Shao, T.S. Park, Dipeptidyl peptidase IV inhibitor attenuates kidney injury in streptozotocin-induced diabetic rats, *J. Pharmacol. Exp. Ther.* 340 (2012) 248–255, <http://dx.doi.org/10.1124/jpet.111.186866>.
- [25] W.J. Liu, M.-N. Luo, J. Tan, W. Chen, L. Huang, C. Yang, Q. Pan, B. Li, H. Liu, Autophagy activation reduces renal tubular injury induced by urinary proteins, *Autophagy* 10 (2014) 243–256, <http://dx.doi.org/10.4161/autophagy.27004>.
- [26] A. Vinaiphat, S. Aluksanasuwan, J. Manissorn, S. Sutthimethakorn, V. Thongboonkerd, Response of renal tubular cells to differential types and doses of calcium oxalate crystals: integrative proteome network analysis and functional investigations, *Proteomics* 17 (2017), <http://dx.doi.org/10.1002/pmic.201700192>.
- [27] Y. Li, M.C. McLaren, K.E. McMartin, Involvement of urinary proteins in the rat strain difference in sensitivity to ethylene glycol-induced renal toxicity, *Am. J. Physiol. Ren. Physiol.* 299 (2010) F605–F615, <http://dx.doi.org/10.1152/ajprenal.00419.2009>.
- [28] D.J. Klionsky, K. Abdelmohsen, A. Abe, et al., Guidelines for the use and interpretation of assays for monitoring autophagy (3rd edition), *Autophagy* 12 (2016) 1–222, <http://dx.doi.org/10.1080/15548627.2015.1100356>.
- [29] S. Kimura, T. Noda, T. Yoshimori, Dissection of the autophagosome maturation process by a novel reporter protein, tandem fluorescent-tagged LC3, *Autophagy* 3 (2007) 452–460.
- [30] G. Gobe, D. Crane, Mitochondria, reactive oxygen species and cadmium toxicity in the kidney, *Toxicol. Lett.* 198 (2010) 49–55, <http://dx.doi.org/10.1016/j.toxlet.2010.04.013>.
- [31] S. Granata, A. Dalla Gassa, P. Tomei, A. Lupo, G. Zaza, Mitochondria: a new therapeutic target in chronic kidney disease, *Nutr. Metab.* 12 (2015) 49, <http://dx.doi.org/10.1186/s12986-015-0044-z>.
- [32] S.R. Khan, Role of renal epithelial cells in the initiation of calcium oxalate stones, *Nephron Exp. Nephrol.* 98 (2004) e55–e60, <http://dx.doi.org/10.1159/000080257>.
- [33] J.H. Wiessner, A.T. Hasegawa, L.Y. Hung, G.S. Mandel, N.S. Mandel, Mechanisms of calcium oxalate crystal attachment to injured renal collecting duct cells, *Kidney Int.* 59 (2001) 637–644, <http://dx.doi.org/10.1046/j.1523-1755.2001.059002637.x>.
- [34] A.J. Browne, A. Göbel, S. Thiele, L.C. Hofbauer, M. Rauner, T.D. Rachner, p38 MAPK regulates the Wnt inhibitor Dickkopf-1 in osteotropic prostate cancer cells, *Cell Death Dis.* 7 (2016) e2119, <http://dx.doi.org/10.1038/cddis.2016.32>.
- [35] K. Nishida, O. Yamaguchi, K. Otsu, Crosstalk between autophagy and apoptosis in heart disease, *Circ. Res.* 103 (2008) 343–351, <http://dx.doi.org/10.1161/CIRCRESAHA.108.175448>.
- [36] S. Luo, D.C. Rubinsztein, Apoptosis blocks Beclin 1-dependent autophagosome synthesis: an effect rescued by Bcl-xL, *Cell Death Differ.* 17 (2010) 268–277, <http://dx.doi.org/10.1038/cdd.2009.121>.
- [37] S. Li, H. Li, D. Yang, X. Yu, D.M. Irwin, G. Niu, H. Tan, Excessive autophagy activation and increased apoptosis are associated with palmitic acid-induced cardiomyocyte insulin resistance, *J. Diabetes Res.* 2017 (2017) 2376893, <http://dx.doi.org/10.1155/2017/2376893>.
- [38] W.-Y. Kim, S.A. Nam, H.C. Song, J.S. Ko, S.H. Park, H.L. Kim, E.J. Choi, Y.-S. Kim, J. Kim, Y.K. Kim, The role of autophagy in unilateral ureteral obstruction rat model, *Nephrol. Carlton Vic.* 17 (2012) 148–159, <http://dx.doi.org/10.1111/j.1440-1797.2011.01541.x>.
- [39] A. Havasi, Z. Dong, Autophagy and tubular cell death in the kidney, *Semin. Nephrol.* 36 (2016) 174–188, <http://dx.doi.org/10.1016/j.semnephrol.2016.03.005>.
- [40] J. Navarro-Yepes, M. Burns, A. Anandhan, O. Khalimonchuk, L.M. del Razo, B. Quintanilla-Vega, A. Pappa, M.I. Panayiotidis, R. Franco, Oxidative stress, redox signaling, and autophagy: cell death versus survival, *Antioxid. Redox Signal.* 21 (2014) 66–85, <http://dx.doi.org/10.1089/ars.2014.5837>.
- [41] T.-H. Chen, P.-C. Chang, M.-C. Chang, Y.-F. Lin, H.-M. Lee, Chloroquine induces the expression of inducible nitric oxide synthase in C6 glioma cells, *Pharmacol. Res.* 51 (2005) 329–336, <http://dx.doi.org/10.1016/j.phrs.2004.10.004>.
- [42] M. Yang, L. Huang, X. Li, E. Kuang, Chloroquine inhibits lytic replication of Kaposi's sarcoma-associated herpesvirus by disrupting mTOR and p38-MAPK activation, *Antivir. Res.* 133 (2016) 223–233, <http://dx.doi.org/10.1016/j.antiviral.2016.08.010>.
- [43] S. Pascolo, Time to use a dose of Chloroquine as an adjuvant to anti-cancer chemotherapies, *Eur. J. Pharmacol.* 771 (2016) 139–144, <http://dx.doi.org/10.1016/j.ejphar.2015.12.017>.